Faraday Discussions

Accepted Manuscript

This manuscript will be presented and discussed at a forthcoming Faraday Discussion meeting. All delegates can contribute to the discussion which will be included in the final volume.

Register now to attend! Full details of all upcoming meetings: http://rsc.li/fd-upcoming-meetings

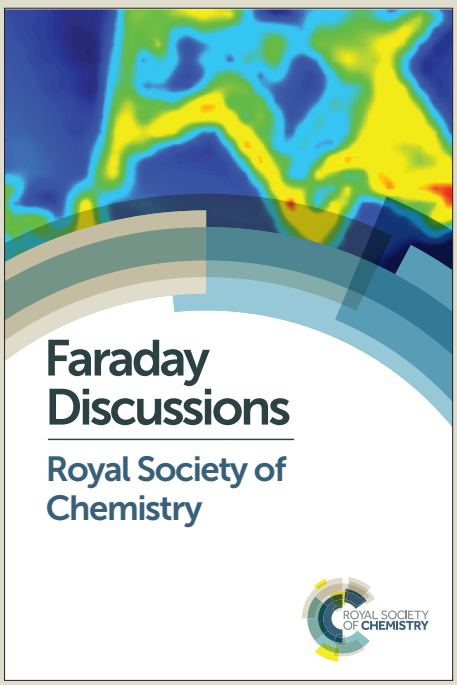

This is an *Accepted Manuscript*, which has been through the Royal Society of Chemistry peer review process and has been accepted for publication.

Accepted Manuscripts are published online shortly after acceptance, before technical editing, formatting and proof reading. Using this free service, authors can make their results available to the community, in citable form, before we publish the edited article. We will replace this *Accepted Manuscript* with the edited and formatted *Advance Article* as soon as it is available.

You can find more information about *Accepted Manuscripts* in the Information for Authors.

Please note that technical editing may introduce minor changes to the text and/or graphics, which may alter content. The journal's standard Terms & Conditions and the Ethical guidelines still apply. In no event shall the Royal Society of Chemistry be held responsible for any errors or omissions in this *Accepted Manuscript* or any consequences arising from the use of any information it contains.

ROYAL SOCIETY OF CHEMISTRY

www.rsc.org/faraday_d

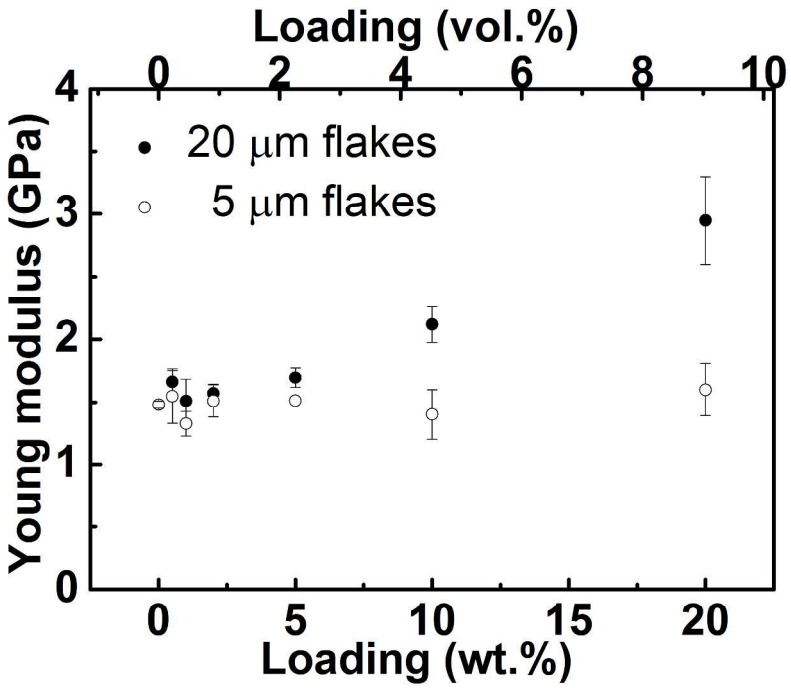

The flake diameter is found to have a critical role in the reinforcement of few-layer graphene - polypropylene composites.
288x201mm (300 x 300 DPI)

Few layer graphene - polypropylene nanocomposites: the role of flake diameter

Cristina Vallés,[a] Amr M. Abdelkader,[a,b] Robert J. Young,[a] and Ian A. Kinloch[a]

DOI: 10.1039/b000000x [DO NOT ALTER/DELETE THIS TEXT]

Graphene shows excellent potential as a structural reinforcement in polymer nanocomposites due its exceptional mechanical properties. We have shown previously that graphene composites can be analysed using conventional composite theory with the graphene flakes acting as short fillers which have a critical length of ~3 μm for good reinforcement. Herein, polypropylene (PP) nanocomposites were prepared using electrochemically-exfoliated-few layer graphene (FLG) with two different flake diameters (5 μm and 20 μm). The crystallization temperature and degree of crystallinity of the PP was found to increase with the loading of FLG, which suggests that the flakes act as crystallisation nucleation sites. Mechanical testing showed that the 5 μm flakes behaved as short fillers and reinforced the PP matrix poorly. The modulus of the 20 μm flake composites, however, increased linearly with loading up to 20 wt.%, without any of the detrimental aggregation effects seen in other graphene systems. The mechanical data were compared with our previous work on other graphene composite systems and the apparent need to balance the degree of functionalization to improve matrix compatibility whilst not encouraging aggregation is discussed.

1 Introduction

Graphene is an atomically-thin, two-dimensional honeycomb material with extraordinary electronic, thermal and mechanical properties [1-3], which makes it an ideal candidate for a wide variety of applications including sensors, batteries, supercapacitors and hydrogen storage [4-7]. A promising application is the incorporation of graphene into polymer matrices in order to improve the electrical, thermal and/or mechanical properties [8-11]. The micromechanics of such graphene composites have been studied extensively by using Raman spectroscopy to probe the behaviour individual flakes of graphene embedded in polymer beams under strain[4, 12, 13]. Examination of the shift rate of the 2D Raman band position with strain has shown that monolayer graphene can achieve an effective modulus of 1 TPa within such polymer composite system[12]. However, this modulus drops as flake becomes thicker due to the internal shear between the graphene layers within the flake, so that a 5 layer flake has a theoretical modulus of 0.6 TPa[14]. This decrease in modulus with thickness would initially suggest that one would use monolayer graphene to reinforce a composite as it has the highest modulus. However, the degree of reinforcement is a function of the loading fraction and modulus. The maximum achievable loading fraction is strongly influenced by the graphene being thinner than the polymer molecules surrounding it; monolayer graphene has a theoretical maximum volume fraction of ~1/7 assuming a perfect dispersion compared to ~1/3 for trilayer graphene. Thus 4-5 layer graphene is the found to be the optimum thickness for reinforcement, taking into account the balance between the increase in volume fraction and drop in modulus with flake thickness. This result is fortuitous as

the majority of scalable graphene production routes produce few layer graphene (FLG).

Micromapping of the Raman spectra within individual flakes has demonstrated that the strain distribution within the flakes can be described by conventional shear lag theory where the strain tends to zero at the edges of the flakes. This phenomenon is known as the "short fibre effect" in fibre composites and states that there is critical length beneath which the end effects dominate and leads to no reinforcement from the filler. Gong *et al.* [12] found that this critical length was ~ 3 µm for unfunctionalised graphene, due to the relatively weak interfacial strength of 1 MPa compared to the 30 MPa found for carbon fibre-epoxy composites. (Graphene has none of the chemical or mechanical interactions of a sized carbon fibre.) Thus, in summary micromechanics predict that ideally a nanocomposite should use FLG typically 4-5 layers thick with a length of > 3 µm, and more preferably > 30 µm.

There is a wide range of literature on the processing and properties of bulk graphene nanocomposites using elastomers, thermosets and thermoplastics[5, 6, 8, 15]. However, most of this literature has used either graphene oxide (GO) or graphite nanoplatelets due to the limited availability of graphene in sufficient scale. Typically these composites show good improvement in the modulus of the composites at very low loadings of graphene (~ 1wt.%), but the degree of reinforcement then falls at higher loadings possibly due to the formation of agglomerates in the polymer matrix.[4, 16] Such aggregation is common in nanomaterial systems due to their high surface area and have been seen in other nanocomposites such as carbon nanotubes. One key difference though between graphene and nanotubes systems is the relatively low viscosity of the platelet systems; carbon nanotubes were ultimately limited in their application due to the viscosity of a nanotube-polymer dispersion increasing to the extent that the dispersion could not be processed by ~ 5 wt.%, whereas herein graphene-related composites have been compounded and injection moulded at loadings of 20 wt.%.

Graphene and graphite nanoplatelets have been found previously to increase the crystallization temperature, crystallization rate, and degree of crystallinity of a PP matrix. It was suggested that the flakes act as a nucleating agent to reduce the barrier to nucleation and modify the crystallite structures of the PP[17-19]. Kalaitzidou et al.[18, 19] found good enhancement of both the mechanical and electrical properties of PP with the addition of exfoliated graphite nanoplatelets at medium loadings (up to 5 vol.%). Functionalization of graphene oxide has also been investigated to improve the dispersion of the flakes in the PP matrix and increase the interfacial adhesion between the filler and the non-polar PP. For example, the reinforcing effects of alkylated graphene oxide (AGO) on a nonpolar PP matrix[20] or the covalently modification of graphene oxide with *p*-phenylenediamine and cyanuric chloride and then grafted with maleic anhydride grafted polypropylene (MAPP)[21] have been studied. Long chain alkylamines with varying chain length have also been chemically grafted to the GO surface in a PP matrix in the presence of maleic anhydride-g-polypropylene (MA-PP) compatibilizer through a melt processing technique[22, 23]. An alternative, more ecologically friendly strategy for nanocomposites has been proposed of first coating graphene with polypropylene (PP) latex and then melt-blending the coated graphene with PP [24]. Significant

improvements in the mechanical and thermal properties of PP were also found by adding only few percent loading of chemically-reduced graphene oxide[25], or polypropylene-graft-reduced graphene oxide (PP-g-rGO) as a novel compatibilizer for PP/polystyrene (PP/PS)[26]. However, even after chemically modifying the surface of the flakes using such approaches, the challenge of achieving good dispersions of the fillers at high loadings limited the properties of the final composites.

Herein, we investigate the effect of flake diameter on the mechanical and thermal properties of bulk PP nanocomposites at loadings relevant to structural applications. Gram quantities of few-layer graphene (FLG) were prepared by reductive electrochemically exfoliation, with the diameter of the flakes being controlled by the graphite grain size in the initial electrode [27]. FLG-PP composites were then prepared from 0.5 to 20 wt.% of two different diameter FLG samples (5 µm and 20 µm) by melt-compounding and followed by injection moulding. The crystallization temperature and degree of crystallization of the PP and the graphene/PP nanocomposites were determined using DSC. The mechanical properties of the composites were evaluated by tensile testing and related to the thermal properties. The effect of exfoliated graphene with different flake sizes as reinforcement in bulk PP composites is then compared with the analogous PMMA composites.

2 Experimental

2.1 Preparation of the graphene and the graphene/PP nanocomposites

Graphene powders with two flake mean sizes, 5 µm (5-FLG) and 20 µm (20-FLG), and similar thickness (< 5 nm) were prepared through a continuous electrochemical exfoliation of graphite, following a procedure described elsewhere by Abdelkader *et al.*[27] All the flakes were under 5 nm in thickness, with ~ 5% of the sheets being monolayer. 5-FLG/PP and 20-FLG/PP composites were prepared with loadings from 0.5 to 20 wt.% by melt mixing using a twin screw extruder. Graphene flakes and PP pellets (Ineos, 100-CA50) were fed into a twin-screw extruder (Thermo Scientific HAAKE MiniLab micro compounder) and the material was cycled for 15 minutes at 190 °C at a screw speed of 100 rpm before being extruded. Extruded samples were further processed into bone shaped specimens by injection moulding (HAAKE MiniJet Piston Injection Moulding System, $C_{ylinder}$ = 190 °C, T_{mould} = 65 °C, Pressure = 740 bar kept for 10 s). Neat PP control samples were processed using the same steps.

2.2 Characterization of the graphene/PP nanocomposites

Scanning electron microscopy (SEM) was used to characterize the morphology and the average lateral diameter of the graphene 5-FLG and 20-FLG flakes using a Philips XL30 FEG SEM, operating at an accelerating voltage of 5 kV.

Differential Scanning Calorimetry (DSC) measurements of the polymer and nanocomposites were carried out under nitrogen gas from 20 °C to 200 °C using a DSC-Q100 from TA Instrument. The samples were first heated to 200 °C at a rate of 10 °C min to remove their thermal history, and after that they were cooled to -40 °C. Both cooling and heating were performed at the same rate of 10 °C min. To determine the crystallization and melting properties the second heating and first cooling cycles were considered. The associated thermal parameters of crystallization (T_c) and melting (Tm) temperatures, crystallization enthalpy (ΔH_c), heat of melting

(ΔH_m), and the percentage of crystallinity (X_c) were extracted. The relative X_c was determined from the melting curves using the following expression:

$$X_C = (\Delta H_m / (1-x)\Delta H_0) \times 100$$

where ΔH_m is the crystallization enthalpy of the samples, ΔH_0 is the theoretical value of the melting heat for a 100 % crystalline PP which is 165 J/g[28], and x is the weight fraction of FLG in the sample.

Stress-strain curves were obtained using dogbone shaped specimens in an Instron 4301 machine, using a tensile rate of 0.5 mm/min with a load cell of 5 kN. The weight fractions were transformed to volume fractions taking the density of the graphene powers as 2.0 g cm^{-3} and that of PP with 51% crystallinity equal to 0.901 g cm^{-3} (the density of amorphous PP, $\rho_{Amorphous}$ = 0.855 g cm^{-3} and that of crystalline PP, $\rho_{crystalline}$ = 0.946 g cm^{-3}).

3 Results and discussion

3.1 Characterization of the graphene flakes

Figure 1 shows micrographs of typical flakes in the 5-FLG and 20-FLG samples. The 5-FLG graphene powder was composed of mainly FLG with a diameter of ~ 5 µm, whereas most of the flakes were ~ 20 µm in diameter in the 20-FLG powder. All the flakes were under 5 nm in thickness, with an average thickness of 2-3 nm and ~ 5 % of the sheets being monolayer[27]. We have found previously with a PMMA system that melt processing of nanocomposites does not significantly reduce these flakes sizes.

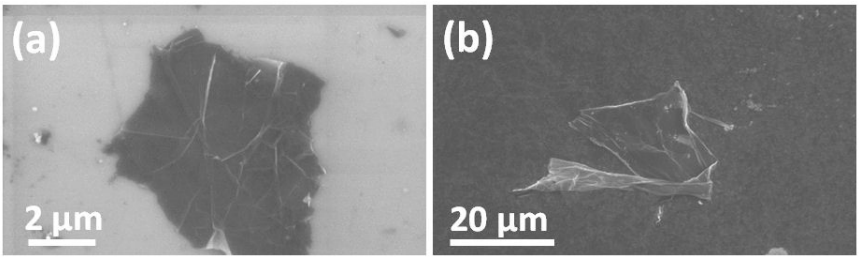

Figure 1 SEM micrographs of the (a) 5-FLG and (b) 20-FLG graphene powders.

3.2 Crystallization and melting properties

The properties, particularly the mechanical properties, of semicrystalline thermoplastic materials are strongly related to their internal microstructure and crystallinity. The crystallization and melting behaviours of the PP matrix were studied under non-isothermal conditions as a function of graphene loading. Figure 2 shows the crystallization and melting curves from the second heating and the first cooling cycles (from DSC) for neat PP and the graphene/PP nanocomposites. The thermal parameters extracted from these curves are summarized in Table 1.

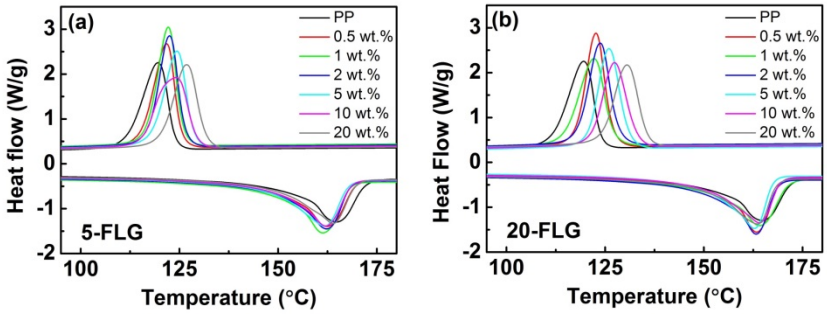

Figure 2 Crystallization thermograms (first cooling cycle) and melting thermograms (second heating cycle) of neat PP and the 5-FLG/PP (a) and 20-FLG (b) nanocomposites.

Table 1 Summarized results of DSC analysis of neat PP and the 5-FLG/PP and 20-FLG/PP nanocomposites with different loadings. (Crystallization, T_c, and melting, T_m, temperatures; crystallization enthalpy, ΔH_c; heat of melting, ΔH_m and the percentage of crystallinity, X_c)) The standard deviation in the values of the temperature were typically less than ± 1 °C from three samples and the standard deviation of the percentage crystallinity were typically less than 1.5.

Sample	wt.%	vol.%	T_c (°C)	ΔH_c (J/g)	T_m (°C)	ΔH_m (J/g)	Xc
5-FLG/PP	0.0	0.0	119.6	97.1	164.8	91.6	55.5
	0.5	0.2	121.8	96.4	162.7	95.4	58.1
	1.0	0.5	122.1	97.6	162.2	99.2	60.7
	2.0	0.9	122.5	94.6	162.3	95.4	59.0
	5.0	2.3	124.3	92.6	161.9	94.4	60.3
	10.0	4.5	124.3	90.5	162.2	91.7	61.2
	20.0	9.0	126.8	86.0	163.9	86.9	65.8
20-FLG/PP	0.0	0.0	119.6	97.1	164.8	91.6	55.5
	0.5	0.2	122.7	94.5	163.4	94.9	57.8
	1.0	0.5	122.4	98.2	163.7	95.1	58.2
	2.0	0.9	123.1	97.1	163.7	96.3	59.5
	5.0	2.3	125.0	94.0	163.1	96.0	61.2
	10.0	4.5	127.8	86.8	164.0	90.3	60.8
	20.0	9.0	129.3	82.8	163.9	86.0	65.1

The crystallisation temperature was found to increase with the addition of the FLG, going from 119.6 °C for pure PP to a maximum temperature of 126.8 °C and 129.3°C for 20 wt.% 5-FLG and 20-FLG graphene, respectively. The degree of crystallinity also increased with the addition of the FLG but the degree of increase was independent of flake diameter, with an increase of ~ 10 % crystallinity observed at 20 wt.% FLG for both diameters. The increases observed in the T_c indicate the

graphene acted as heterogeneous nucleation sites which facilitated the crystallization of PP during cooling. The results from the heating curve (Fig. 2) found similar values for the T_m for both composite systems and the neat PP. For the neat PP, the melting peak at 164.9 °C is attributed to the melting of α-crystals, which is the most common monoclinic crystal structure of PP. (The melting of β-crystals gives a peak at 147.5 °C). The results from the melting curves revealed that no β-crystalline structure is present in the neat PP nor in the graphene/PP nanocomposites. This will be investigated further by X-ray in future work.

3.3 Mechanical properties

All the samples were found to behave as glassy polymers (Fig. 3) with the tensile facture strain decreasing with increasing FLG loading. This embrittlement with the addition of FLG is similar that reported for other nanotubes and graphene composites.[29] The tensile strengths of the 20-FLG remained constant with loading, whereas the tensile strength of the 5-FLG dropped for the medium loaded samples (Fig. 4).

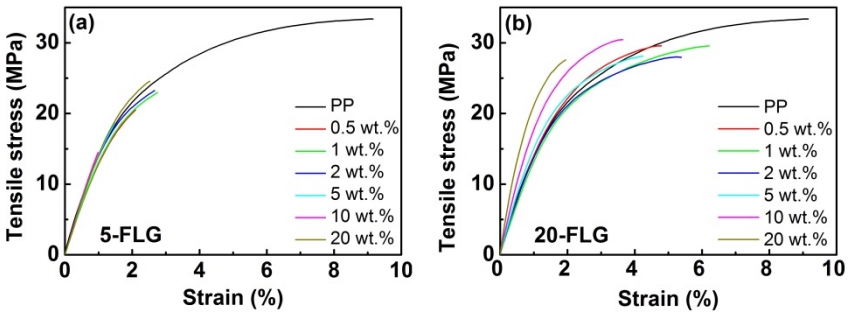

Figure 3 Stress-strain curves of 5-FLG/PMMA (a) and 20-FLG/PMMA (b) Figure 4b shows the values of the Young's modulus (E) determined by tensile testing plotted as a function of the filler content.

There was no significant change within experimental error of the Young's Modulus, *E*, of the 5-FLG/PP composites with loading (Table 2). However, for the 20-FLG/PP composites a linear increase of *E* with loading was observed with the modulus doubling at a 20 wt.% loading (2.95 GPa).

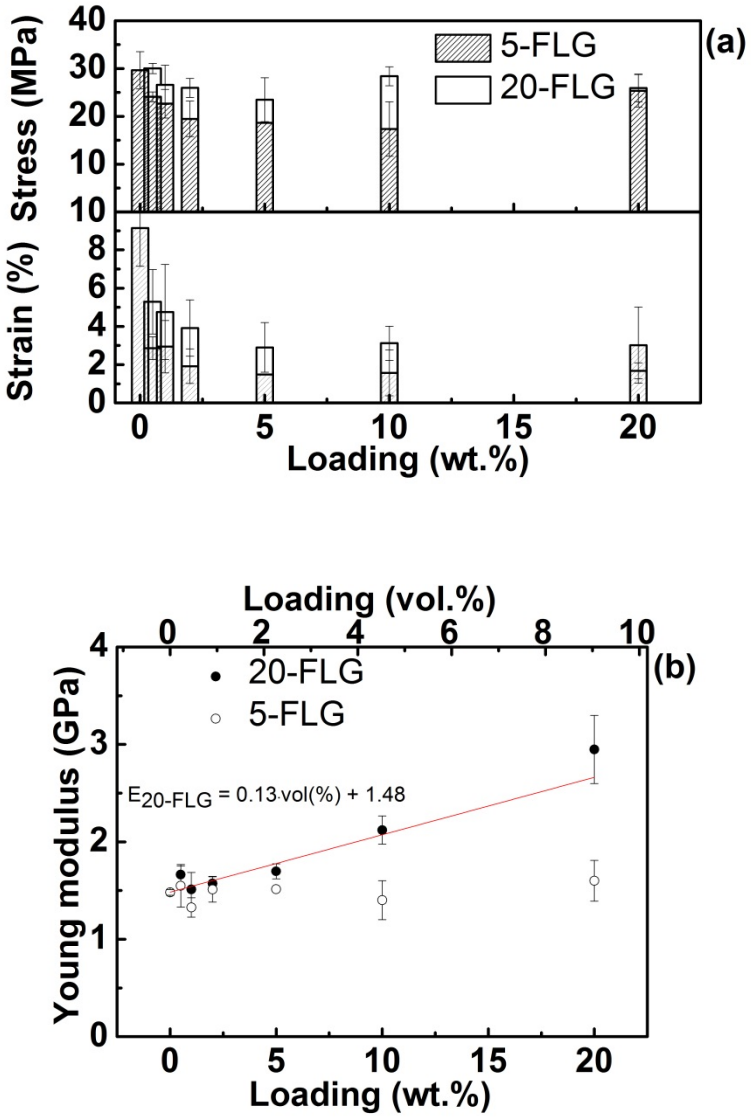

Figure 4 (a) Variation of the strain and stress at break of the composites with loading. (b) Variation of Young's modulus, *E,* with loading for the two series of nanocomposites. Error bars represent the standard deviation calculated from between 4 and 7 samples.

Table 2: The modulus of the composites as a function of loading and flake diameter.

Loading (wt.%)	Loading (vol.%)	E of the composites with:	
		5 µm flakes	20 µm flakes
0.0	0.0	1.5 ± 0.0	1.5 ± 0.0
0.5	0.2	1.5 ± 0.2	1.7 ± 0.1
1.0	0.5	1.3 ± 0.1	1.5 ± 0.2
2.0	0.9	1.5 ± 0.1	1.6 ± 0.1
5.0	2.3	1.5 ± 0.0	1.7 ± 0.1
10.0	4.5	1.4 ± 0.2	2.1 ± 0.1
20.0	9.0	1.6 ±0.2	2.9 ± 0.4

4. Discussion of the mechanical properties of graphene reinforced thermoplastics

4.1 Discussion of the PP system

The mechanical properties of the composites are strongly related to the morphology of polymer and any reinforcement from the filler. If as seen herein, the addition of the filler induces crystallization then reinforcement from both the change in polymer morphology and the FLG need to be considered[30]. In general the nucleation of PP crystals and an increase in crystallinity will lead to an increase in the Young's modulus and yield stress of the PP matrix and possible reduce the elongation at failure[31, 32]. Fortunately, both the 5-FLG and 20-FLG composite systems had a similar change in crystallinity (10 %), allowing effect of crystallinity to be separated from the flake diameter. Given the 5-FLG composites had a constant modulus with loading, it could be assumed that the neither the small increase in crystallinity nor the flakes significantly reinforced the polymer. Thus the increase in modulus for the 20 µm flakes can be approximated to be entirely from the contribution of the larger flakes.

The Young's modulus, E_C, of a particulate composite, in the case of uniform strain (and assuming good dispersions of graphene at loadings below the optimal), is given by the modified rule of mixtures as:

$$E_C = E_p \cdot V_p \eta_0 \eta_l + E_m \cdot V_m$$

where E_p is the Young's modulus of the particles, E_m is the Young's modulus of the polymer matrix, and V_p and V_m are the volume fractions of particles and matrix, respectively, within the composites. η_0 is the Krenchal orientation factor and depends on the average orientation of the particles to the stress. η_l is also between 0 and 1 and adjusts for the poor stress transfer arising from poor interfaces and/or short fibers, with 1 being a continuous fibre. Frequently the effective modulus, E_{eff}, of a particle is considered which is given by η_l x E_p as it is frequently not possible to separate the two values in a bulk system.

For the 5 μm flakes (5-FLG) there was no reinforcement as the flakes were behaving as short fibres, hence η_l and E_{eff} are equal to 0. For the 20 μm flakes (20-FLG) $E_{\text{eff}} \cdot \eta_0$ can be estimated from the gradient of the E vs volume fraction, which gives a value of 13 GPa. We have previously used polarised Raman spectroscopy to assess the degree of orientation in PMMA-FLG injection moulded composites and found that it was random due to the relatively low shear in the small scale injection moulding machine. We therefore assume that the PP composites also have randomly aligned flakes, thus the we can take η_0 as ~ 3/8 (the Krenchel factor for a random 2D orientation of the graphene flakes), leading a value of 35 GPa for the 20 μm flakes, compared to predicted theoretical maximum of ~600 GPa[14].

3.4 Comparison with previously studied systems

Figure 5 summarises our studies to-date on thermoplastic (semi-crystalline PP and amorphous poly methyl acrylate, PMMA) using FLG and graphene oxide (GO) as reinforcements with the modulus normalised to that of the matrix being used. The steeper the slope of the graph the high the effective modulus of the graphene, as in the more reinforcement is achieved per flake in the system. However, the ultimate performance of the composite also matters at useful loadings; there is little application value in a composite system which has outstanding reinforcement at low loadings (e.g. < 5 wt.%) and then does not improve in its absolute properties at higher loadings (e.g. 20-30 wt.%.) Thus the ideal composite system in Figure 5 would have a high gradient and linearly increase across all volume fractions, without levelling off.

The importance of having a sufficiently large diameter flake is demonstrated for the electrochemically exfoliated FLG in both the PP and PMMA systems, with the 5 μm diameter flakes showing little or no improve in the modulus up to 20 wt.% loading. However, 20 μm diameter flakes did show linearly improvements in both systems, with the highest degree of reinforcement in PP, possibly due to the increase in the crystallinity. So far it was the literature has tended to show that good reinforcement were only found at relatively low levels of graphene loading due the reason being given as obtaining a good dispersion at the higher loadings[4]. Obtaining a good distribution of the nano-reinforcement is one of the greatest challenges in the preparation of polymer-based nanocomposites[33] since it will be demonstrated that the properties of the nanocomposites can be compromised by a poor dispersion. Herein we show the achievement of good mechanical properties for high volume fractions of unfunctionalized graphene.

GO is frequently used as a reinforcement in polymers because it offers two important advantages with respect to "clean" graphene: i) frequent production in high yield and scale and ii) the presence of a high number of oxygen-containing functionalities providing a good dispersion of the flakes in the matrix at low concentrations through electrostatic dispersion and enhanced graphene-polymer interaction. In particular, the surface chemistry allows shorter flakes to be used as the critical length is dependent on the interfacial shear strength, which depends on the matrix-polymer interaction. (For example the GO flakes used here are < 10 μm in diameter.) As shown on Figure 5, the surface chemistry does lead to a higher

degree of reinforcement than the FLG at low loadings, due to the homogeneous distribution of the flakes in the polymer. The effect modulus values at these loadings are in the range of 200-300 GPa in total agreement with values determined theoretically that can be found in the literature. However, at higher loadings of graphene oxide however the mechanical properties were found to deteriorate due to the formation of agglomerates of graphene oxide, possibly as the GO flakes get close enough to enter the deep energy minimum for electrostatic dispersions where agglomerates are formed.

This comparison of GO and FLG highlights the key challenges now facing the field; functionalization definitely improves the interface of graphene, improving the interface sufficiently to compensate for the drop in the modulus which the functionalization causes. (The modulus is inversely related to the cross-sectional area of the flake and the functional groups significant increase the cross-sectional area of an atomically thin material, which is the predominant reason why the modulus of monolayer GO is less than that of monolayer graphene.) However, in most cases to date, the functionalization of graphene appears to increase the rate of aggregation compared to unfunctionalized graphene. Thus a balance of the degree and type of functionalization is required, possibility using steric groups to increase the matrix interface and prevent further aggregation.

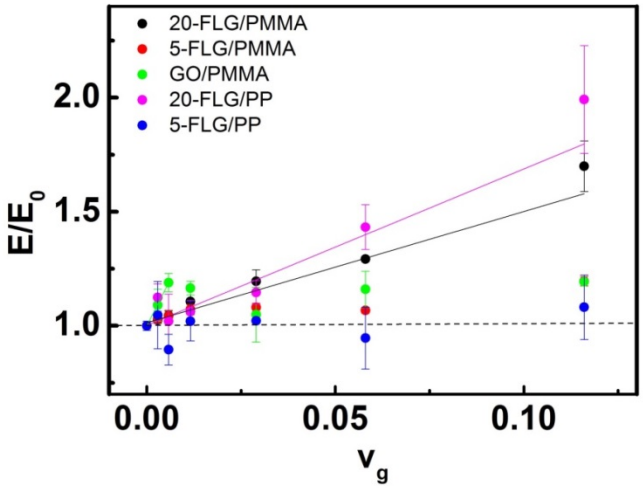

Figure 5 Variation of E/E_0 with loading for different graphene/polymer systems. Error bars represent the standard deviation calculated from between 4 and 7 samples.

4 Conclusions

Electrochemically exfoliated few layer graphene with two different diameters (5 µm and 20 µm) and similar thickness were incorporated in a PP matrix by melt mixing using a twin screw extruder at loadings from 0 to 20 wt.% followed by injection

moulding. Increases in the crystallization temperature and degree of crystallinity with loading were found for the two sizes of graphene, which suggested that the flakes are acting as nucleation sites for the polymer. Mechanical testing showed that the 5 μm flakes behaved as short fibres and poorly reinforced the PP matrix compared to the 20 μm flakes, in line with previous predictions on the critical length of graphene. Significantly, these larger flakes gave a linear increase in the modulus even at high loadings, without any of the detrimental aggregation effects seen in most other graphene systems. This short fibre effect found in the graphene/PP system was in agreement with a previously studied graphene/PMMA system. The FLG-based systems were also compared with previously reported graphene oxide-based systems. The graphene oxide was found to provide a stronger interface with the polymer relative to the unfunctionalized or ”clean” graphene, giving high levels of reinforcement up to relatively low optimal loadings. At higher loadings the formation of agglomerates of graphene oxide in the matrix causes the mechanical properties of the material to deteriorate.

It is unlikely that graphene will compete with carbon fibre reinforced plastic (CFRP) composites in the near term due to the high degree of orientation and loading of carbon in the CRFP. However, the modulus of the unoptimised 9 vol % 20-FLG PP composite is the same as that of the corresponding randomly orientated E-glass fibre composite as flakes are more efficient at forming isotropic systems than fibres. However, the FLG system weighs 6 % less due to the low density of carbon. Therefore it plausible that with future work on sizing the FLG, graphene is a viable competitor to injection moulded glass-fibre composites for mass produced products.

Acknowledgements

The authors are grateful to the EPSRC (Grants No: EP/I023879/1 and EP/K016946/1).

[a] *School of Materials, University of Manchester, Oxford Road, Manchester, M13 9PL, UK*
Tel: 0161 3063615; E-mail: ian.kinloch@manchester.ac.uk
[b] *School of Chemistry, University of Manchester, Oxford Road, Manchester, M13 9PL, UK*

References

1. S. Park and R. S. Ruoff, *Nat Nanotechnol*, 2009, **4**, 217-224.

2. A. K. Geim, *Science*, 2009, **324**, 1530-1534.

3. A. K. Geim and K. S. Novoselov, *Nat Mater*, 2007, **6**, 183-191.

4. R. J. Young, I. A. Kinloch, L. Gong and K. S. Novoselov, *Compos Sci Technol*, 2012, **72**, 1459-1476.

5. R. Verdejo, M. M. Bernal, L. J. Romasanta and M. A. Lopez-Manchado, *J Mater Chem*, 2011, **21**, 3301-3310.

6. V. Singh, D. Joung, L. Zhai, S. Das, S. I. Khondaker and S. Seal, *Prog Mater Sci*, 2011, **56**, 1178-1271.

7. S. Stankovich, D. A. Dikin, G. H. B. Dommett, K. M. Kohlhaas, E. J. Zimney, E. A. Stach, R. D. Piner, S. T. Nguyen and R. S. Ruoff, *Nature*, 2006, **442**, 282-286.

8. H. Kim, A. A. Abdala and C. W. MacOsko, *Macromolecules*, 2010, **43**, 6515-6530.

9. X. Huang, X. Qi, F. Boey and H. Zhang, *Chemical Society Reviews*, 2012, **41**, 666-686.

10. J. R. Potts, D. R. Dreyer, C. W. Bielawski and R. S. Ruoff, *Polymer*, 2011, **52**, 5-25.

11. R. J. Young and I. A. Kinloch, in *Nanoscience: Volume 1: Nanostructures through Chemistry*, The Royal Society of Chemistry, 2013, pp. 145-179.

12. L. Gong, I. A. Kinloch, R. J. Young, I. Riaz, R. Jalil and K. S. Novoselov, *Adv Mater*, 2010, **22**, 2694-2697.

13. T. M. G. Mohiuddin, A. Lombardo, R. R. Nair, A. Bonetti, G. Savini, R. Jalil, N. Bonini, D. M. Basko, C. Galiotis, N. Marzari, K. S. Novoselov, A. K. Geim and A. C. Ferrari, *Physical Review B*, 2009, **79**, 205433.

14. L. Gong, R. J. Young, I. A. Kinloch, I. Riaz, R. Jalil and K. S. Novoselov, *ACS Nano*, 2012, **6**, 2086-2095.

15. T. K. Das and S. Prusty, *Polymer - Plastics Technology and Engineering*, 2013, **52**, 319-331.

16. Z. Li, R. J. Young and I. A. Kinloch, *ACS Applied Materials and Interfaces*, 2013, **5**, 456-463.

17. C. I. Ferreira, C. Dal Castel, M. A. S. Oviedo and R. S. Mauler, *Thermochimica Acta*, 2013, **553**, 40-48.

18. K. Kalaitzidou, H. Fukushima, P. Askeland and L. Drzal, *J Mater Sci*, 2008, **43**, 2895-2907.

19. K. Kalaitzidou, H. Fukushima and L. T. Drzal, *Composites Part A: Applied Science and Manufacturing*, 2007, **38**, 1675-1682.

20. Y. S. Yun, Y. H. Bae, D. H. Kim, J. Y. Lee, I.-J. Chin and H.-J. Jin, *Carbon*, 2011, **49**, 3553-3559.

21. B. Yuan, C. Bao, L. Song, N. Hong, K. M. Liew and Y. Hu, *Chemical Engineering Journal*, 2014, **237**, 411-420.

22. S. H. Ryu and A. M. Shanmugharaj, *Materials Chemistry and Physics*, 2014.

23. S. H. Ryu and A. M. Shanmugharaj, *Chemical Engineering Journal*, 2014, **244**, 552-560.

24. P. Song, Z. Cao, Y. Cai, L. Zhao, Z. Fang and S. Fu, *Polymer*, 2011, **52**, 4001-4010.

25. M. El Achaby, F. E. Arrakhiz, S. Vaudreuil, A. El Kacem Qaiss, M. Bousmina and O. Fassi-Fehri, *Polym Compos*, 2012, **33**, 733-744.

26. F. You, D. Wang, X. Li, M. Liu, Z. M. Dang and G. H. Hu, *Journal of Applied Polymer Science*, 2014, **131**.

27. A. M. Abdelkader, I. A. Kinloch and R. A. W. Dryfe, *ACS Applied Materials & Interfaces*, 2014, **6**, 1632-1639.

28. J. E. Mark, *New York, Oxford University Press*, 1999.

29. J. Yang, X. Yan, M. Wu, F. Chen, Z. Fei and M. Zhong, *J Nanopart Res*, 2012, **14**.

30. J. N. Coleman, M. Cadek, R. Blake, V. Nicolosi, K. P. Ryan, C. Belton, A. Fonseca, J. B. Nagy, Y. K. Gun'ko and W. J. Blau, *Advanced Functional Materials*, 2004, **14**, 791-798.

31. Y. Mubarak, P. J. Martin and E. Harkin-Jones, *Plastics, Rubber and Composites Processing and Applications*, 2000, **29**, 307-315.

32. F. Stan, L. I. Sandu and C. Fetecau, *Composites Part B: Engineering*, 2014, **59**, 109-122.

33. M. Moniruzzaman and K. I. Winey, *Macromolecules*, 2006, **39**, 5194-5205.